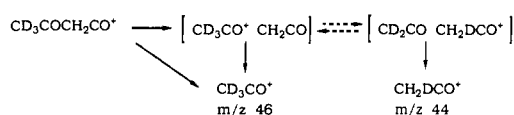


Scheme VII



under the final state. Moreover, by invoking tunnelling effects, described elsewhere<sup>15a</sup> in this kind of linear C-H-C structure, the barrier of 21 kJ mol<sup>-1</sup> could be an upper limit for the hydrogen transfer.

The energy diagram elaborated at MP2/6-31+G\*\*//6-31G\* with these different data (Figure 4) is in accordance with the experimental results.

As the transition state for H transfer is below the final state, the isomerization leading to atom exchange is observed. However, its energy being very near that of the final state, the competition between the simple cleavage of **1** and the isomerization strongly depends on several parameters. On the one hand, this explains the low ratio of atom exchange in stable ions as previously shown in the CAD spectra of labeled ions **1**. This result accounts for the strong primary isotope effect when a deuterium atom is involved in the transfer **10** → **10'**: the abundance of *m/z* 46 (CD<sub>3</sub>CO<sup>+</sup>) peak in the MIKE spectrum of **1c** indicates that D transfer is inhibited, whereas the shape of this peak (existence of three components) shows that the direct cleavage of the initial ion becomes competitive in this case (Scheme VII).

### Conclusion

Metastable CH<sub>3</sub>COCH<sub>2</sub>CO<sup>+</sup> cation reacts via intermediate complexes. These complexes are not simply proton-bound dimers

of ketene [O=C=CH<sub>2</sub>...H<sup>+</sup>...CH<sub>2</sub>=C=O]. The symmetric structure in which a proton is bonded to two neutral ketene corresponds to a transition state. Instead, the intermediate corresponds to weakly bonded complexes of the form [acylium ketene].

Several stable structures have been considered. They are stabilized by different effects: weak bonding between a hydrogen atom of the acylium and the oxygen (or the carbon) of the ketene or interaction between a positive charge and a basic carbon. For this reason, the interconversion among structures is easy. One moiety can turn with respect to the other right below the threshold for dissociation, even though the intermolecular distances remain short.

Structure **7**, in which one hydrogen of the acylium is bonded to a ketene oxygen, is the most stable form of the [acylium ketene] complex but cannot lead to atom exchange reaction. The reactive structures are higher in energy and lie near the transition state. This implies that the calculation of a strongly stabilized structure cannot be the only argument to justify the intermediacy of a complex.

Only the energy variation has been discussed in this work. Entropy variation has been neglected in the first approximation. The study of substituted ions **1**, which will be published elsewhere, shows that this level of description is not always sufficient.

**Supplementary Material Available:** Tables of total energies (in hartrees) and relative energies (in kJ mol<sup>-1</sup>) on selected levels of theory (2 pages). Ordering information is given on any current masthead page.

## Experimental and Theoretical Studies of Alkaline-Earth Metal Coordination: X-ray Crystal Structures of Calcium, Strontium, and Barium Carbazoles and ab Initio Model Calculations

Gabriele Mösges,<sup>†</sup> Frank Hampel, Martin Kaupp, and Paul von Ragué Schleyer\*

Contribution from the Institut für Organische Chemie, Friedrich-Alexander Universität Erlangen-Nürnberg, Henkestrasse 42, D-8520 Erlangen, Germany. Received September 19, 1991

**Abstract:** The solid-state structures of the aromatic alkaline-earth metal amides (*N*-carbazolyl)<sub>2</sub>Ca(pyridine)<sub>4</sub> (**1**), (*N*-carbazolyl)<sub>2</sub>Sr(NH<sub>3</sub>)(DME)<sub>2</sub> (**2**) (DME = 1,2-dimethoxyethane), and (*N*-carbazolyl)<sub>2</sub>Ba(DME)<sub>3</sub> (**3**) are compared. Compounds **1–3** crystallize as monomers with the M<sup>2+</sup> cation (M = Ca, Sr, Ba) σ-bound to the carbazole nitrogen atoms. This is in contrast to the dimeric alkali metal carbazoles, which exhibit varying degrees of polyhaptic bonding to the carbazole π-system. While the metal coordination smoothly increases from six to seven to eight with M = Ca, Sr, Ba, respectively, the orientation of the anionic carbazole ligands changes from cisoid with M = Ca, Sr to transoid with M = Ba. Ab initio calculations on a series of solvated and unsolvated model complexes indicate this to be due to covalent Ba–N σ-bonding contributions involving metal d-orbitals and to cation polarization. These factors favor bent X–Ba–X arrangements, both in “naked” BaX<sub>2</sub> compounds and in solvated complexes BaX<sub>2</sub>(L)<sub>n</sub>. Anion–anion repulsion prevents cisoid structures for the complexes of the smaller Ca and Sr cations. Crystal data for **1**: monoclinic space group *P*2<sub>1</sub>/*c*, *Z* = 4, *a* = 12.723 (6) Å, *b* = 18.169 (13) Å, *c* = 22.348 (10) Å, β = 105.82 (4)°. Crystal data for **2**: monoclinic space group *Cc*, *Z* = 4, *a* = 15.910 (9) Å, *b* = 13.040 (4) Å, *c* = 16.522 (7) Å, β = 116.83 (3)°. Crystal data for **3**: monoclinic space group *P*2<sub>1</sub>/*c*, *Z* = 4, *a* = 9.785 (6) Å, *b* = 27.071 (7) Å, *c* = 14.370 (4) Å, β = 109.58 (4)°.

### Introduction

What factors govern the coordination chemistry of the heavier alkaline earth metals? Theoretical studies of a large number of MX<sub>2</sub> compounds (M = Ca, Sr, Ba, Sm, Eu, Yb; X = H, Li, BeH,

BH<sub>2</sub>, CH<sub>3</sub>, NH<sub>2</sub>, OH, Halogen, η<sup>5</sup>-C<sub>5</sub>H<sub>5</sub>) demonstrate that, apart from pure Coulomb-type interactions, the influence of covalent bonding contributions involving metal d-orbitals, and the high polarizabilities of these heavy-metal cations are involved.<sup>1–5</sup> While

<sup>†</sup> In memoriam (February 21, 1964 to February 16, 1992).

(1) Kaupp, M.; Schleyer, P. v. R.; Stoll, H.; Preuss, H. *J. Chem. Phys.* 1991, 94, 1360.

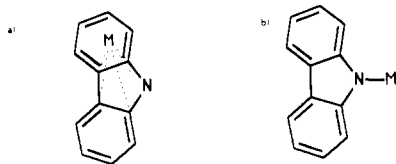


**Figure 1.** Schematic representation of (a) multihapto  $\pi$ - ("cyclopentadienyllithium-like") bonding and (b) monohapto  $\sigma$ -bonding (amide-like).<sup>7</sup>

the energetic contributions of these effects to binding are relatively small, they may lead to a preference for significantly bent  $\text{MX}_2$  structures<sup>1-5</sup> and even to substantial rotational barriers in diamides.<sup>4</sup>

In our continuing attempts to increase the understanding of group 2 structural chemistry, we now compare the X-ray crystal structures of the organic diamides (*N*-carbazolyl)<sub>2</sub>Ca(pyridine)<sub>4</sub> (1), (*N*-carbazolyl)<sub>2</sub>Sr(NH<sub>3</sub>)(DME)<sub>2</sub> (2), and (*N*-carbazolyl)<sub>2</sub>Ba(DME)<sub>3</sub> (3) (DME = 1,2-dimethoxyethane).

There are several questions of interest: What aggregation do the alkaline-earth metal carbazoles prefer (the alkali metal carbazoles are dimers<sup>6</sup>)? What are the coordination numbers at the metal? What is the orientation of the anionic ligands, cisoid or transoid? Do the heavier alkaline-earth metal carbazoles prefer "cyclopentadienyllithium-like" structures<sup>7</sup> or  $\sigma$ -bonded amide arrangements (cf. Figure 1)?

Although an organometallic complex of the alkaline-earth element calcium was reported over 80 years ago,<sup>8</sup> the structural chemistry of the organic compounds of calcium, strontium, and barium remains undeveloped.<sup>9</sup> One of the major problems is the insolubility of the simple alkyl, aryl, or alkenyl complexes in common organic solvents. Therefore, the structurally characterized "true" organometallics (i.e., the metal is bound to carbon) almost exclusively contain cyclopentadienyl ligands, either substituted or unsubstituted.<sup>9</sup> The recently obtained structure of {Ca[CH(SiMe<sub>3</sub>)<sub>2</sub>]<sub>2</sub>(1,4-dioxane)<sub>2</sub>} is a notable exception.<sup>10</sup>

Only few organic amides of the heavier alkaline-earth metals have been investigated. The molecular structure of a mixed imino derivative of aluminum and calcium [(*t*-C<sub>4</sub>H<sub>9</sub>Na)(H)<sub>3</sub>(*t*-C<sub>4</sub>H<sub>9</sub>NCa)](THF)<sub>3</sub> has been characterized by Cuccinella.<sup>11</sup> Six structures containing the N(SiMe<sub>3</sub>)<sub>2</sub> group are known: The dimers {M[N(SiMe<sub>3</sub>)<sub>2</sub>]<sub>2</sub>}<sub>2</sub> (M = Ca,<sup>12</sup> Sr,<sup>13</sup> Ba<sup>14</sup>) and {Ba[N(SiMe<sub>3</sub>)<sub>2</sub>]<sub>2</sub>(THF)<sub>2</sub>}<sub>2</sub> exhibit bridging N(SiMe<sub>3</sub>)<sub>2</sub> units. Monomeric Ca[N(SiMe<sub>3</sub>)<sub>2</sub>]<sub>2</sub>(DME)<sup>12</sup> has a distorted tetrahedral geometry. The recently published X-ray structure of polymeric

{*trans*-Sr[N(SiMe<sub>3</sub>)<sub>2</sub>]<sub>2</sub>( $\mu$ -1,4-dioxane)}<sub>n</sub> shows a remarkable square-planar coordination of strontium.<sup>10</sup> Miculcik et al. obtained X-ray structures of the monomeric complexes (2-mercaptobenzoxazole)<sub>2</sub>Ba(HMPPTA)<sub>3</sub> [HMPPTA = O=P(NMe<sub>2</sub>)<sub>3</sub>] and (2-mercaptobenzoxazole)<sub>2</sub>Ca(HMPPTA)<sub>2</sub>(H<sub>2</sub>O)<sub>2</sub>.<sup>15</sup>

To help the interpretation of the experimentally observed structural data, we have performed ab initio quantum chemical calculations on a variety of model systems. The question, whether the factors that favor the inherently bent structures of "naked" BaX<sub>2</sub> species<sup>1-5</sup> give rise to related effects in solvated complexes (i.e. a preference for cisoid anionic ligands), is investigated by pseudopotential calculations on the six-coordinate model compounds M(NH<sub>2</sub>)<sub>2</sub>(HF)<sub>4</sub> (M = Ca, Ba). To obtain insight into the relative multihapto vs monohapto preferences of the heavier group 1 and 2 cations to carbazolyl or related ligands, we have calculated a series of unsolvated systems XM<sup>+</sup>po<sup>-</sup> (XM<sup>+</sup> = Na<sup>+</sup>, K<sup>+</sup>, Cs<sup>+</sup>, Ca<sup>+</sup>, Ba<sup>+</sup>, HCa<sup>+</sup>, FCa<sup>+</sup>, HBa<sup>+</sup>; po<sup>-</sup> = pyrrole anion, C<sub>4</sub>H<sub>4</sub>N<sup>-</sup>).

#### Details of the ab Initio Pseudopotential Calculations

Quasirelativistic multi-electron-fit 9-valence-electron (K, Cs)<sup>16</sup> and 10-valence-electron pseudopotentials (Ca, Ba)<sup>1</sup> were employed for the heavier metals. A 1-valence-electron pseudopotential was used for Na,<sup>17</sup> and the 1s-shells for carbon, nitrogen, and fluorine also were replaced by effective core potentials.<sup>18,19</sup> Full Hartree-Fock geometry optimizations of the pyrrole complexes XM<sup>+</sup>po<sup>-</sup> were carried out with [6s6p1d]/(4s4p1d) valence basis sets for K and Cs,<sup>16,20</sup> [6s6p5d]/(6s6p2d) sets for Ca and Ba,<sup>1</sup> [4s4p1d]/(2s2p1d) for Na,<sup>20,21a</sup> and [5s5p1d]/(3s3p1d) bases including diffuse and polarization functions for C, N, and F.<sup>3,20-22</sup> In the HF-optimizations of M(NH<sub>2</sub>)<sub>2</sub>(HF)<sub>4</sub> (M = Ca, Ba), the diffuse and polarization functions on N and F have been omitted (this basis set combination will be designated as basis A). Dunning and Hay's [4s]/(2s) basis<sup>23</sup> was used for hydrogen. Open shell systems (XM<sup>+</sup>po<sup>-</sup>; XM<sup>+</sup> = Ca<sup>+</sup>, Ba<sup>+</sup>) have been calculated within the unrestricted Hartree-Fock (UHF) scheme.

Four conformations have been considered for each of the two model complexes M(NH<sub>2</sub>)<sub>2</sub>(HF)<sub>4</sub> (M = Ca, Ba): Two structures with the amide groups in *cis* position (one eclipsed with the amide hydrogens in the N-M-N plane, cf. Figures 2a and 3a, and one staggered, cf. Figures 2b and 3b), and the corresponding two *trans* geometries (Figures 2c,d and 3c,d) were calculated. The M-F-H angles have been restricted to 180° to exclude intramolecular hydrogen bonding. All other geometry parameters have been optimized within the given point group (C<sub>s</sub> for the staggered and C<sub>2v</sub> for the eclipsed structures). Additional MP2 single-point calculations at the SCF-optimized geometries have been performed to obtain the relative energies of the different structures. These calculations employed a slightly decontracted (311) metal d-basis and one additional metal f-function,<sup>1</sup> as well as diffuse and polarization functions on N and F.<sup>3,20,22</sup> This basis set will be designated as basis B.

In preliminary tests, we tried to use H<sub>2</sub>O as a model coligand instead of HF. However, it has been impossible to exclude intramolecular hydrogen bonding interactions either between the different water ligands or between NH<sub>2</sub> and H<sub>2</sub>O groups. As these

(2) Seijo, L.; Barandiaran, Z.; Huzinaga, S. *J. Chem. Phys.* **1991**, *94*, 3762.

(3) Kaupp, M.; Schleyer, P. v. R.; Stoll, H.; Preuss, H. *J. Am. Chem. Soc.* **1991**, *113*, 6012.

(4) Kaupp, M.; Schleyer, P. v. R. *J. Am. Chem. Soc.* **1992**, *114*, 491.

(5) Kaupp, M.; Schleyer, P. v. R.; Dolg, M.; Stoll, H. Submitted to *J. Am. Chem. Soc.*

(6) (a) Gregory, K. Dissertation, Universität Erlangen-Nürnberg, 1991.

(b) Hacker, R.; Kaufmann, E.; Schleyer, P. v. R.; Mahdi, W.; Dietrich, H. *Chem. Ber.* **1987**, *120*, 1533. (c) Gregory, K. Diplomarbeit, Universität Erlangen-Nürnberg, 1988. (d) Gregory, K.; Bremer, M.; Schleyer, P. v. R.; Klusener, P. A. A.; Brandsma, L. *Angew. Chem.* **1990**, *101*, 1261.

(7) (a) Setzer, W.; Schleyer, P. v. R. *Adv. Organomet. Chem.* **1985**, *24*, 353. (b) Schade, C.; Schleyer, P. v. R. *Adv. Organomet. Chem.* **1988**, *27*, 169.

(8) Beckmann, E. *Chem. Ber.* **1905**, *38*, 904.

(9) (a) Lindsell, W. E. In *Comprehensive Organometallic Chemistry*; Wilkinson, G., Stone, F. G. A., Abel, G., Eds.; Pergamon Press: Oxford, England, 1982; Vol. 1, Chapter 4. (b) Hanusa, T. P. *Polyhedron* **1990**, *9*, 1345. (c) The recently obtained crystal structure of the bis-fluorenyl complex BaF<sub>2</sub>(NH<sub>3</sub>)<sub>4</sub> may also be considered as a substituted cyclopentadienyl system: Mösseg, G.; Hampel, F.; Schleyer, P. v. R. *Organometallics* **1992**, *11*, 1170.

(10) Geoffrey, F.; Cloke, N.; Hitchcock, P. B.; Lappert, M. F.; Lawless, G. A.; Royo, B. *J. Chem. Soc., Chem. Commun.* **1991**, 724.

(11) Cuccinella, S.; Dozzi, G.; Perego, G.; Mazzei, A. *J. Organomet. Chem.* **1977**, *137*, 257.

(12) Westerhausen, M.; Schwarz, W. Z. *Anorg. Allg. Chem.* **1991**, *604*, 127.

(13) Westerhausen, M.; Schwarz, W. Z. *Anorg. Allg. Chem.* **1991**, *606*, 177.

(14) Vaartstra, B. A.; Huffman, J. C.; Streib, W. E.; Caulton, K. G. *Inorg. Chem.* **1991**, *30*, 121.

(15) Mikulcik, P.; Raithby, P. R.; Snaith, R.; Wright, D. S. *Angew. Chem.* **1991**, *103*, 452.

(16) Küchle, W.; Bergner, A.; Dolg, M.; Stoll, H.; Preuss, H. Unpublished results.

(17) Fuentealba, P.; v. Szentpály, L.; Preuss, H.; Stoll, H. *J. Phys. B* **1985**, *73*, 1287.

(18) Igel-Mann, G.; Stoll, H.; Preuss, H. *Mol. Phys.* **1988**, *65*, 1321.

(19) Dolg, M. Dissertation, Universität Stuttgart, 1989.

(20) The d-polarization functions were taken from: *Gaussian Basis Sets for Molecular Calculations*; Huzinaga, S., Ed.; Elsevier: New York, 1984.

(21) (a) Poppe, J.; Igel-Mann, G.; Savin, A.; Stoll, H. Unpublished results. (b) Kaupp, M.; Stoll, H.; Preuss, H. *J. Comput. Chem.* **1990**, *11*, 1029.

(22) Clark, T.; Chandrasekhar, J.; Spitznagel, G. W.; Schleyer, P. v. R. *J. Comput. Chem.* **1983**, *4*, 294.

(23) Dunning, T. H.; Hay, P. J. In *Methods of Electronic Structure Theory*; Theoretical Chemistry, Vol. 3; Schaefer, H. F., III, Ed.; Modern Theoretical Chemistry, Vol. 3; Plenum Press: New York, 1977.

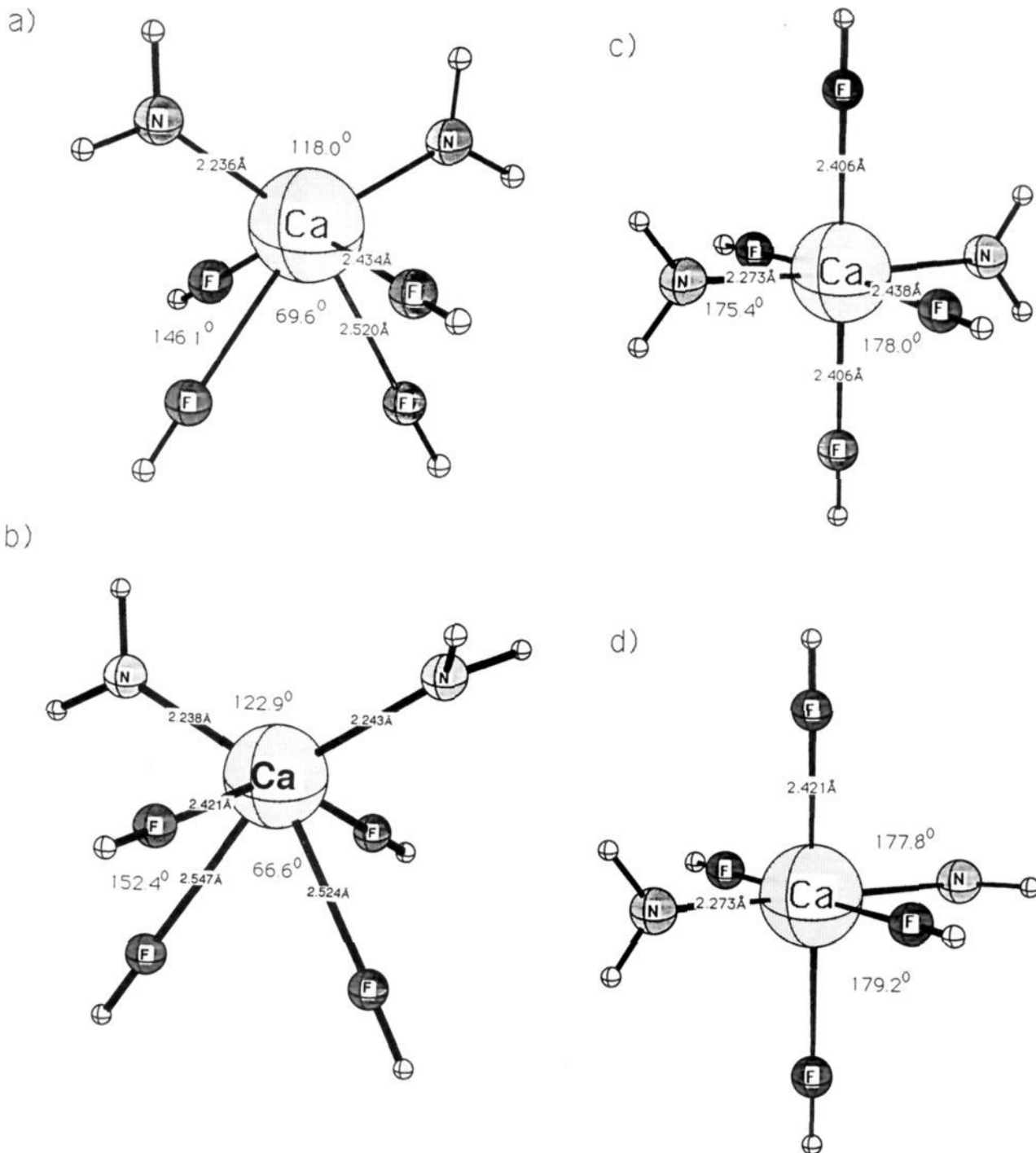


**Figure 2.** Structures considered for the model complex  $\text{Ca}(\text{NH}_2)_2(\text{HF})_4$ : (a) cis/eclipsed; (b) cis/staggered; (c) trans/eclipsed; (d) trans/staggered.

contributions are most pronounced for the cis structures, the stability of these configurations, compared to that of the trans geometries, tends to be overestimated (assuming that this type of hydrogen bonding is absent in the systems we intend to model). With HF (in the linear arrangement described above), both the geometries obtained and the Reed–Weinhold natural population analyses<sup>24</sup> indicate these effects to be negligible. HF is a slightly weaker donor ligand than  $\text{H}_2\text{O}$  or most of the organic solvents employed as neutral coligands in Ca, Sr, or Ba coordination chemistry. Nevertheless, we expect these model systems to be sufficiently realistic to draw quite general conclusions.

(24) Reed, A. E.; Weinstock, R. B.; Weinhold, F. *J. Chem. Phys.* **1985**, *83*, 735.

Two structures have been considered for each of the model complexes  $\text{XM}^+\text{po}^-$ : a multihapto  $C_s$  geometry with the  $\text{XM}^+$  fragment in a plane perpendicular to the pyrrole ring (see, e.g., Figure 4a for the  $\text{HBa}^+$  complex) and a geometry with  $\text{XM}^+$   $\sigma$ -bound to the nitrogen atom. The latter structure was optimized within  $C_{2v}$  symmetry; i.e., the pyrrole unit was taken to be planar and an X–M–N angle of  $180^\circ$  (for  $\text{XM}^+ = \text{HCa}^+$ ,  $\text{FCa}^+$ ,  $\text{HBa}^+$ ) was imposed (cf. Figure 4b). Additional, less restricted, calculations have been performed for  $\text{XM}^+ = \text{HBa}^+$ , as the bending of related  $\text{XBaX}$  species may lead to stabilizations of several kcal/mol compared to linear arrangements.<sup>1,3–5</sup> Thus, the H–Ba–N angle was allowed to vary, but the hydrogen atom was restricted to be in the barium–pyrrole plane. This results in a full optimization within  $C_s$  symmetry (cf. Figure 4c). Preliminary

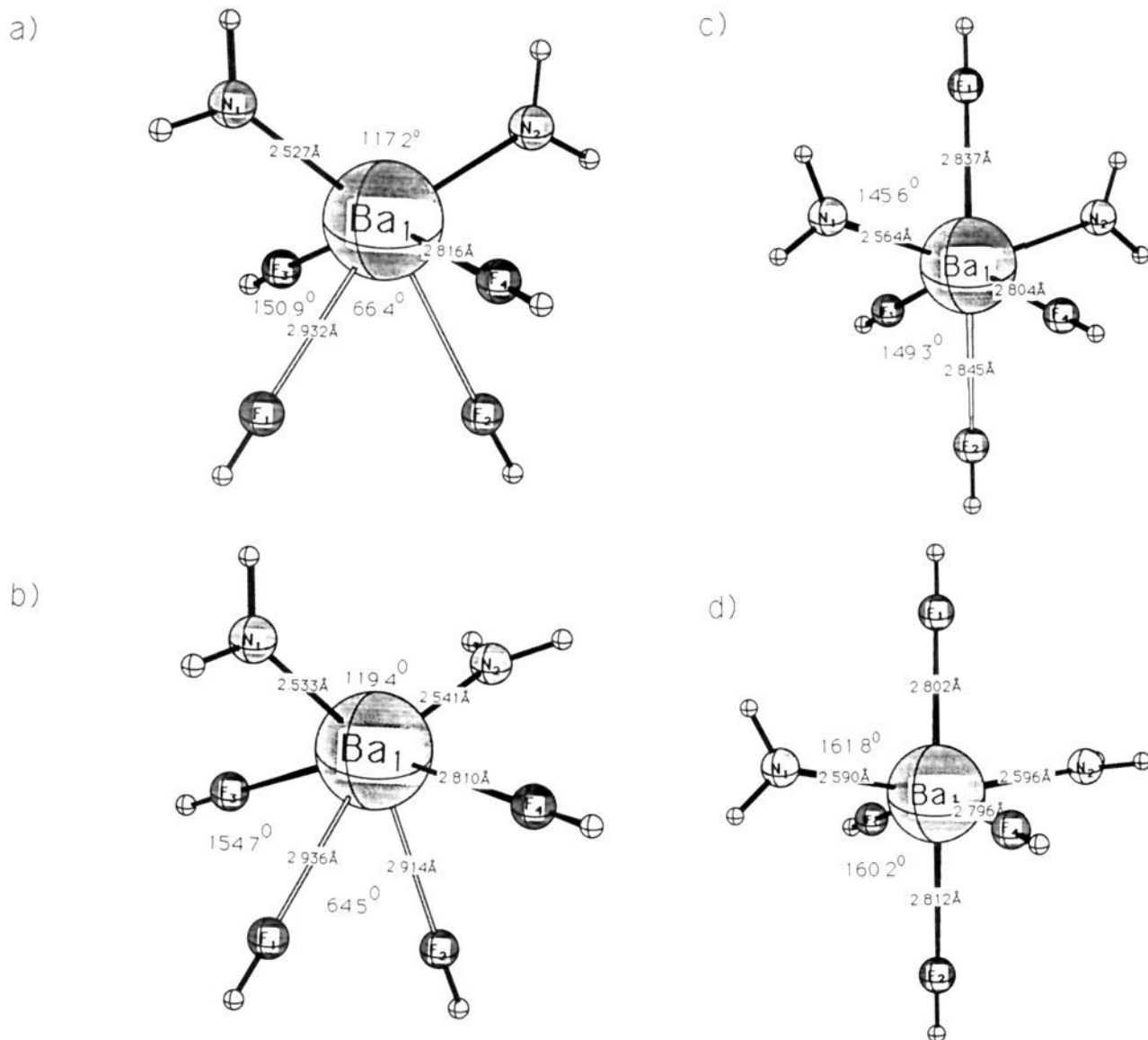


**Figure 3.** Structures considered for the model complex  $\text{Ba}(\text{NH}_2)_2(\text{HF})_4$ : (a) cis/eclipsed; (b) cis/staggered; (c) trans/eclipsed; (d) trans/staggered.

geometry optimizations (omitting the diffuse and polarization functions on C and N) showed this "in-plane"  $C_s$  structure to be ca 1.5 kcal/mol more stable than an "out-of-plane"  $C_s$  arrangement with the hydrogen atom in a plane perpendicular to the pyrrole ring (but without multihapto bonding to the ring  $\pi$ -system). This conformational preference has been observed previously for  $\text{Ba}(\text{NH}_2)_2$  and is due to ligand-to-metal  $\pi$ -bonding contributions.<sup>4</sup> No bent monohapto structure was calculated for  $\text{XM}^+ = \text{HCa}^+$ ,  $\text{FCa}^+$ , as the bending effects are known to be small for  $\text{CaX}_2$  compounds.<sup>1-5</sup>

The effects of electron correlation on the metal-pyrrole distances and on the multihapto vs monohapto stabilities have been considered at the MP2 level of theory. The metal-ring centroid distances in the multihapto species and the M-N distances in the monohapto structures were optimized by single-point MP2 calculations and a quadratic fit. The other geometry parameters were kept fixed at their Hartree-Fock values. Larger metal basis sets have been employed for these MP2 calculations: [7s7p2d]/(5s5p2d) sets<sup>16,20</sup> were used for K and Cs. The Ca and Ba basis sets were uncontracted to (6s6p3d) and augmented by one f-function.<sup>1</sup> The Na basis set was uncontracted (3s2p1d). All electrons outside the pseudopotential cores were correlated at the MP2 level.

All ab initio calculations have been performed with the Gaussian 90 program.<sup>25</sup> Natural population analyses (NPA)<sup>24</sup> were carried

out with the Gaussian 90 adaptation of the NBO program.

## Results

**X-ray Structure of (*N*-Carbazolyl)<sub>2</sub>Ca(pyridine)<sub>4</sub> (1).** In the solid state, **1** is a hexacoordinated monomer with nearly perfect octahedral ligand symmetry (cf. Figure 5 and Table I). The asymmetric unit includes three additional pyridine molecules which are not bound to the calcium atom. The two carbazole substituents, situated in apical positions, are twisted relative to one another. Four pyridine molecules complete the calcium coordination sphere.

The Ca-N (carbazole) bond lengths, 2.438 and 2.448 Å, are somewhat shorter than the bridging Ca-N distances in  $[\text{Ca}[\text{N}(\text{SiMe}_3)_2]_2]_2$  (2.49 Å)<sup>12</sup> and in the hexacoordinate  $[(t\text{-C}_4\text{H}_9\text{NAlH})_3(t\text{-C}_4\text{H}_9\text{NCa})](\text{THF})_3$  (2.49 Å).<sup>11</sup> The Ca-N (pyridine) bond lengths range from 2.514 to 2.54 Å. There is no detectable interaction between the  $\text{Ca}^{2+}$  cation and the  $\pi$ -face of the carbazole system. Table II provides the fractional coordinates and isotropic temperature factors.

(25) Frisch, M. J.; Head-Gordon, M.; Trucks, G. W.; Foresman, J. B.; Schlegel, H. B.; Raghavachari, K.; Robb, M.; Binkley, J. S.; Gonzalez, C.; DeFrees, D. J.; Fox, D. J.; Whiteside, R. A.; Seeger, R.; Melius, C. F.; Baker, J.; Kahn, L. R.; Stewart, J. J. P.; Topiol, S.; Pople, J. A. *Gaussian 90*; Gaussian, Inc.: Pittsburgh, PA, 1990; Revision F.

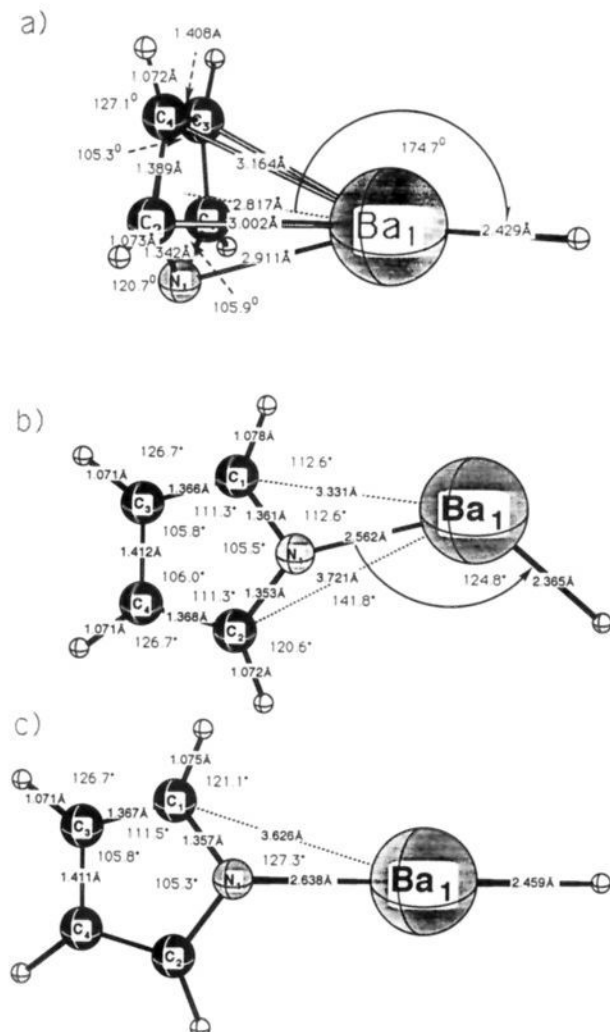


**Figure 4.** HF-optimized structures of  $\text{HBa}^+\text{po}^-$ : (a) multi-hapto structure; (b) monohapto, linear  $C_{2v}$  structure; (c) monohapto, bent  $C_{2v}$  structure.

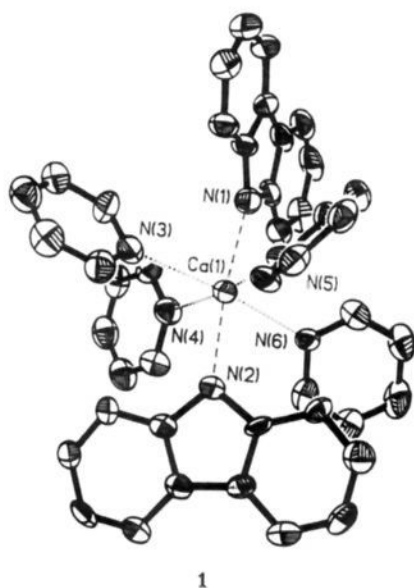


**Figure 5.** X-ray crystal structure of **1**.

**X-ray Structure of  $(N\text{-Carbazolyl})_2\text{Sr}(\text{NH}_3)(\text{DME})_2$  (**2**).** ( $N\text{-Carbazolyl})_2\text{Sr}(\text{NH}_3)(\text{DME})_2$  (**2**) to our knowledge is the first

**Table I.** Selected Bond Lengths (Å) and Angles (deg) in the Alkaline-Earth Metal Carbazole Complexes **1**, **2**, and **3**

	<b>1</b> M = Ca L = pyridine	<b>2</b> M = Sr L = DME, $\text{NH}_3$	<b>3</b> M = Ba L = DME
Bond Lengths			
M-N(1)	2.438	2.615	2.749
M-N(2)	2.448	2.565	2.752
M-N(3)	2.514	2.674	
M-N(4)	2.540		
M-N(5)	2.524		
M-N(6)	2.520		
M-O(1)		2.555	2.868
M-O(2)		2.608	2.803
M-O(3)		2.638	2.834
M-O(4)		2.718	2.921
M-O(6)			2.834
M-O(7)			2.935
Bond Angles			
N(1)-M-N(2)	172.7	171.3	98.1
N(3)-M-N(6)	172.1		
N(4)-M-N(5)	173.3		
N(1)-M-N(3)		84.9	
N(1)-M-O(1)		95.0	136.6
N(1)-M-O(2)		77.8	78.9
N(1)-M-O(3)		103.4	142.8
N(1)-M-O(4)		80.0	104.3
N(1)-M-O(5)			83.5
N(1)-M-O(6)			73.8

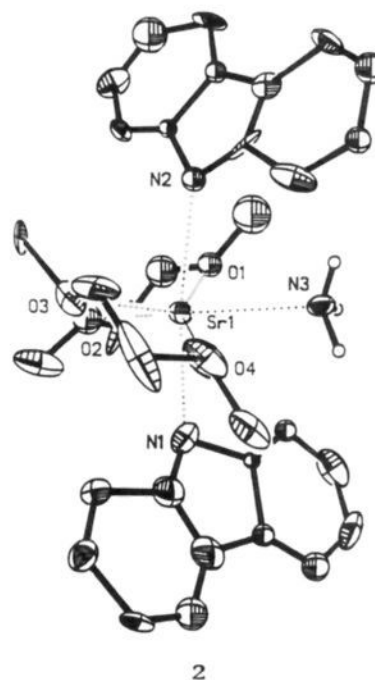


**Figure 6.** X-ray crystal structure of **2**.

structurally characterized aromatic strontium amide. The structural features of **2** (cf. Figure 6 and Table I) are similar to those of **1**. Compound **2** also crystallizes as a monomer. Two carbazoles, two chelating DME ligands, and one ammonia molecule lead to a coordination number of seven with a distorted pentagonal-bipyramidal environment for strontium.

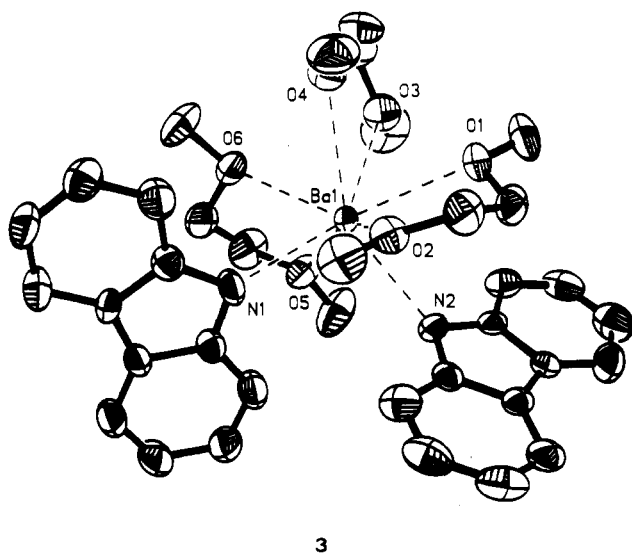
The two apical carbazole anions in **2** are similarly twisted as in **1**. The coordination of one ammonia molecule is an unusual feature in this type of complex. Apparently, this is due to the availability of an additional coordination site for a small monodentate ligand. The Sr-N (carbazole) bond lengths are 2.615 and 2.565 Å (note that the Sr-N(2) distance is not refined anisotropically); they are slightly shorter than those of the N-Sr-N bridge (2.65 Å) in  $[\text{Sr}[\text{N}(\text{SiMe}_3)_2]_2]_2$ .<sup>13</sup> The Sr-N (ammonia)

Table II. Fractional Coordinates ( $\times 10^4$ ) and Isotropic Thermal Parameters ( $U(\text{eq})$  in  $\text{pm}^2 \times 10^{-2}$ ) for **1**, **2**, and **3** ( $U = 1/3(U_{11} + U_{22} + U_{33})$ )

	x	y	z	$U(\text{eq})$		x	y	z	$U(\text{eq})$
<b>1</b>									
Ca(1)	865 (1)	2523 (1)	1765 (1)	32 (1)	C(41)	3398 (7)	2420 (4)	543 (4)	57 (4)
N(1)	-907 (5)	2560 (3)	992 (2)	38 (2)	C(42)	2828 (8)	2145 (4)	-33 (4)	57 (4)
C(1)	-1860 (6)	2167 (4)	974 (3)	34 (3)	C(43)	1737 (8)	2001 (4)	-141 (4)	53 (4)
C(2)	-1999 (6)	1601 (4)	1384 (3)	42 (3)	C(44)	1214 (7)	2141 (4)	317 (4)	49 (4)
C(3)	-3008 (7)	1284 (4)	1294 (4)	56 (4)	N(5)	-172 (5)	2528 (3)	2581 (3)	37 (2)
C(4)	-3872 (7)	1497 (5)	794 (4)	64 (5)	C(50)	265 (6)	2192 (4)	3119 (4)	40 (3)
C(5)	-3746 (7)	2028 (5)	394 (4)	56 (4)	C(51)	-260 (7)	2143 (4)	3584 (3)	44 (4)
C(6)	-2746 (6)	2393 (4)	479 (3)	41 (3)	C(52)	-1283 (7)	2454 (4)	3498 (4)	49 (4)
C(7)	-2334 (7)	2955 (4)	174 (4)	42 (4)	C(53)	-1736 (6)	2807 (4)	2952 (4)	43 (4)
C(8)	-2800 (7)	3391 (5)	-348 (4)	58 (4)	C(54)	-1173 (6)	2824 (3)	2504 (3)	39 (3)
C(9)	-2173 (8)	3907 (5)	-539 (4)	62 (5)	N(6)	1131 (5)	3895 (3)	1729 (3)	37 (3)
C(10)	-1074 (7)	3981 (4)	-236 (3)	50 (4)	C(60)	307 (7)	4378 (4)	1665 (3)	49 (4)
C(11)	-577 (7)	3544 (4)	280 (3)	45 (4)	C(61)	451 (7)	5127 (4)	1759 (4)	56 (4)
C(12)	-1228 (6)	3031 (4)	490 (3)	38 (3)	C(62)	1521 (9)	5390 (5)	1936 (4)	69 (5)
N(2)	2523 (4)	2552 (3)	2634 (2)	30 (2)	C(63)	2372 (7)	4907 (4)	1998 (3)	57 (4)
C(13)	2794 (6)	3108 (4)	3076 (3)	31 (3)	C(64)	2138 (7)	4172 (4)	1880 (3)	45 (4)
C(14)	2075 (6)	3621 (4)	3229 (3)	39 (3)	C(70)	2814 (9)	83 (6)	359 (5)	83 (6)
C(15)	2540 (7)	4174 (4)	3657 (3)	49 (4)	C(71)	3247 (8)	219 (5)	969 (6)	79 (5)
C(16)	3664 (7)	4202 (4)	3958 (3)	47 (4)	C(72)	3235 (8)	-314 (7)	1373 (4)	82 (5)
C(17)	4350 (6)	3687 (4)	3823 (3)	40 (3)	N(7)	2777 (8)	-980 (5)	1202 (5)	81 (5)
C(18)	4400 (5)	2564 (4)	3116 (3)	33 (3)	C(74)	2380 (9)	-1074 (5)	604 (6)	76 (6)
C(19)	5474 (6)	2310 (4)	3201 (3)	44 (3)	C(75)	2390 (8)	-571 (7)	177 (5)	82 (5)
C(20)	5665 (6)	1741 (4)	2852 (4)	54 (4)	C(80)	2305 (9)	674 (6)	4611 (6)	98 (6)
C(21)	4819 (7)	1389 (4)	2408 (4)	50 (4)	C(81)	3298 (12)	600 (6)	5043 (5)	106 (7)
C(22)	3746 (6)	1624 (4)	2320 (3)	39 (3)	N(8)	4215 (10)	929 (5)	4916 (5)	135 (7)
C(23)	3918 (6)	3140 (4)	3382 (3)	31 (3)	C(83)	3985 (9)	1320 (5)	4362 (5)	75 (5)
C(24)	3527 (6)	2219 (4)	2668 (3)	30 (3)	C(84)	2951 (9)	1362 (4)	4000 (4)	59 (4)
N(3)	813 (6)	1140 (3)	1732 (3)	42 (3)	C(82)	2140 (6)	1050 (4)	4121 (4)	47 (4)
C(30)	1272 (6)	691 (5)	2204 (4)	51 (4)	C(90)	3681 (9)	-509 (7)	3613 (4)	75 (5)
C(31)	1194 (7)	-65 (5)	2172 (4)	58 (4)	C(94)	3561 (10)	-1215 (8)	3606 (5)	98 (6)
C(32)	646 (8)	-379 (5)	1620 (5)	64 (5)	C(92)	4094 (13)	-1649 (6)	3300 (7)	121 (8)
C(33)	159 (7)	55 (5)	1127 (4)	64 (4)	C(93)	4785 (10)	-1295 (10)	2986 (6)	119 (8)
C(34)	276 (7)	808 (5)	1204 (4)	52 (4)	N(9)	4912 (8)	-574 (7)	3014 (4)	101 (5)
N(4)	1757 (5)	2400 (3)	882 (3)	42 (3)	C(95)	4357 (10)	-213 (5)	3316 (5)	79 (6)
C(40)	2821 (6)	2543 (4)	975 (3)	45 (3)					
<b>2</b>									
Sr(1)	0	1079 (1)	0	22 (1)	C(18)	-1742 (15)	2297 (14)	1426 (10)	26 (5)
N(1)	833 (13)	1153 (13)	-1019 (11)	37 (5)	C(19)	-2381 (13)	1557 (14)	927 (12)	17 (4)
C(1)	1744 (17)	942 (17)	-691 (14)	42 (7)	C(20)	-3396 (13)	1434 (16)	570 (13)	36 (6)
C(2)	2170 (14)	-72 (14)	-105 (11)	30 (6)	C(21)	-3737 (19)	487 (19)	-11 (17)	52 (7)
C(3)	3109 (17)	-181 (16)	146 (14)	38 (8)	C(22)	-3266 (16)	-81 (16)	-241 (14)	37 (7)
C(4)	3720 (14)	599 (16)	-69 (15)	36 (6)	C(23)	-2277 (16)	112 (13)	140 (13)	33 (8)
C(5)	3244 (15)	1343 (17)	-634 (14)	38 (5)	C(24)	-1857 (12)	855 (13)	645 (11)	13 (3)
C(6)	2317 (18)	1542 (17)	-918 (14)	40 (6)	N(3)	-101 (15)	3148 (4)	26 (15)	33 (4)
C(7)	1657 (14)	2347 (14)	-1553 (11)	19 (4)	O(1)	-1739 (9)	1460 (9)	-1360 (8)	25 (3)
C(8)	1741 (16)	3154 (16)	-1993 (14)	34 (6)	C(25)	-2407 (19)	2089 (18)	-1317 (16)	63 (7)
C(9)	924 (19)	3718 (17)	-2510 (16)	46 (7)	C(26)	-2135 (14)	666 (16)	-1983 (14)	45 (6)
C(10)	147 (14)	3433 (14)	-2459 (13)	48 (6)	C(27)	-1400 (18)	23 (13)	-2059 (13)	71 (12)
C(11)	-38 (14)	2666 (12)	-2026 (11)	20 (4)	O(2)	-769 (11)	-411 (11)	-1122 (10)	38 (4)
C(12)	751 (10)	2129 (10)	-1516 (9)	18 (3)	C(28)	-244 (15)	-1166 (18)	-1212 (15)	62 (8)
N(2)	-920 (11)	1271 (11)	966 (10)	21 (3)	O(3)	797 (12)	-422 (11)	1184 (9)	46 (5)
C(13)	-917 (12)	2024 (12)	1473 (11)	33 (4)	C(29)	48 (16)	-1192 (13)	1185 (15)	55 (9)
C(14)	-103 (16)	2691 (17)	1967 (14)	49 (7)	C(30)	1315 (14)	17 (15)	2004 (12)	51 (9)
C(15)	-80 (12)	3562 (12)	2529 (11)	21 (3)	C(31)	2079 (16)	645 (17)	1969 (13)	77 (8)
C(16)	-1021 (16)	3740 (17)	2477 (14)	34 (5)	O(4)	1603 (10)	1519 (12)	1340 (10)	57 (5)
C(17)	-1803 (17)	3161 (16)	1988 (14)	36 (6)	C(32)	2333 (15)	2139 (16)	1215 (14)	47 (6)
<b>3</b>									
Ba(1)	392 (1)	6321 (1)	2665 (1)	29 (1)	C(21)	-2005 (10)	8447 (3)	1763 (7)	74 (4)
N(1)	2593 (6)	5850 (2)	2231 (4)	46 (2)	C(22)	-2637 (8)	7991 (3)	1578 (6)	62 (3)
C(1)	3295 (7)	5417 (2)	2575 (5)	42 (3)	C(23)	-1848 (7)	7563 (3)	1605 (5)	48 (3)
C(2)	3538 (8)	5199 (3)	3509 (5)	55 (3)	C(24)	-328 (7)	7612 (2)	1833 (4)	34 (2)
C(3)	4285 (8)	4747 (3)	3715 (5)	53 (3)	C(25)	-1199 (9)	7188 (3)	4130 (6)	67 (4)
C(4)	4820 (8)	4526 (3)	3040 (6)	56 (3)	O(1)	148 (5)	6965 (2)	4187 (3)	50 (2)
C(5)	4597 (8)	4735 (3)	2109 (5)	52 (3)	C(26)	1291 (9)	7309 (3)	4483 (5)	56 (3)
C(6)	3836 (7)	5184 (2)	1884 (5)	35 (2)	C(27)	2707 (9)	7044 (3)	4860 (5)	59 (3)
C(7)	3442 (6)	5503 (2)	1046 (5)	35 (2)	O(2)	2830 (5)	6681 (2)	4169 (3)	46 (2)
C(8)	3679 (8)	5503 (3)	141 (5)	56 (3)	C(28)	4274 (8)	6500 (3)	4418 (6)	68 (3)
C(9)	3166 (9)	5892 (3)	-496 (6)	65 (4)	C(29)	-3609 (9)	6205 (4)	2019 (8)	100 (5)
C(10)	2409 (8)	6285 (3)	-260 (5)	58 (3)	O(3)	-2349 (5)	6162 (2)	2881 (4)	59 (2)
C(11)	2166 (8)	6290 (3)	620 (5)	53 (3)	C(30)	-2489 (10)	5763 (3)	3497 (8)	82 (5)
C(12)	2695 (7)	5900 (2)	1304 (5)	39 (2)	C(31)	-1291 (11)	5795 (3)	4450 (7)	80 (5)
N(2)	674 (5)	7237 (2)	1919 (4)	34 (2)	O(4)	64 (6)	5756 (2)	4309 (4)	60 (2)
C(13)	1971 (7)	7480 (2)	2153 (4)	34 (2)	C(32)	1236 (10)	5791 (3)	5211 (6)	82 (4)
C(14)	3356 (8)	7272 (3)	2338 (5)	53 (3)	C(33)	-1756 (11)	6524 (3)	-96 (6)	88 (4)
C(15)	4539 (8)	7582 (3)	2597 (5)	60 (3)	O(5)	-1166 (6)	6158 (2)	638 (3)	53 (2)
C(16)	4376 (9)	8097 (4)	2647 (5)	63 (3)	C(34)	-1646 (10)	5675 (3)	259 (6)	70 (4)
C(17)	3058 (8)	8308 (3)	2466 (5)	51 (3)	C(35)	-709 (9)	5296 (3)	911 (6)	59 (3)
C(18)	1821 (7)	7999 (2)	2224 (4)	36 (2)	O(6)	-745 (6)	5348 (2)	1879 (4)	57 (2)
C(19)	325 (7)	8089 (2)	2020 (4)	37 (2)	C(36)	-200 (10)	4911 (2)	2447 (7)	76 (4)
C(20)	-525 (9)	8511 (3)	1999 (6)	61 (3)					

**Table III.** Summary of Crystallographic Data for Compounds 1, 2, and 3

	1	2	3
emp form.	C <sub>59</sub> H <sub>51</sub> N <sub>9</sub> Ca	C <sub>37</sub> H <sub>39</sub> N <sub>3</sub> O <sub>4</sub> Sr	C <sub>36</sub> H <sub>44</sub> BaN <sub>2</sub> O <sub>6</sub>
color, habit	yellow rhombs	colorless rhombs	colorless rhombs
cryst size (mm)	0.3 × 0.4 × 0.5	0.3 × 0.3 × 0.3	0.25 × 0.4 × 0.4
cryst syst	monoclinic	monoclinic	monoclinic
space group	P2 <sub>1</sub> /c	Cc	P2 <sub>1</sub> /c
unit cell			
<i>a</i> (Å)	12.723	15.910	9.785
<i>b</i> (Å)	18.169	13.040	27.071
<i>c</i> (Å)	22.348	16.522	14.370
$\alpha$ (deg)	90.0	90.0	90.0
$\beta$ (deg)	105.82	116.83	109.58
$\gamma$ (deg)	90.0	90.0	90.0
Vol (Å <sup>3</sup> )	4970	3060	3586
<i>Z</i>	4	4	4
$\rho_z$ (g cm <sup>-3</sup> )	1.238	1.340	1.371
$\mu$ (mm <sup>-1</sup> )	0.168	1.802	1.149
<i>F</i> (000)	1952	1288	1520
diffractometer		Nicolet R 3m/V	
radiation		Mo K $\alpha$	
temp (K)		200	
monochromator		highly oriented graphite crystal	
2 $\theta$ range (deg)		3.0–55.0	
scan type		$\omega$	
scan range	1.40 ( $\omega$ )	0.7 ( $\omega$ )	0.70 ( $\omega$ )
scan speed		variable, 3.00–14.66 deg/min in $\omega$	
std refls		3 measured every 100 reflections	
indep refls	10443	5563	7891
obsd refls	3833 ( $F > 6.0\sigma(F)$ )	3525 ( $F > 6.0\sigma(F)$ )	5493 ( $F > 4.0\sigma(F)$ )
solution		direct methods (SHELXTL PLUS 4.11/V)	
refinement		full-matrix least-squares	
quantity minimized		$\sum \omega(F_o - F_c)^2$	
hydrogen atoms		riding model, fixed isotropic <i>U</i>	
weighting scheme		$\omega^{-1} = \sigma^2(F) + 0.0001F^2$	
<i>R</i>	0.0906	0.0662	0.0607
<i>R</i> <sub>w</sub>	0.0603	0.0549	0.0492
data/parameter	6.2:1	12.6:1	13.5:1

**Figure 7.** X-ray crystal structure of 3.

distance is 2.674 Å. Sr–O (DME) distances range from 2.555 to 2.718 Å. Again, only  $\sigma$ -bonding to the carbazole nitrogens is found. The fractional coordinates and the isotropic temperature factors are given in Table II.

**X-ray Structure of (*N*-Carbazolyl)<sub>2</sub>Ba(DME)<sub>3</sub> (3).** The X-ray structure reveals a monomer with features similar to 1 and 2 (cf. Figures 5–7, Table I). However, the orientation of the carbazoles in 3 (cisoid) notably differs from those in 1 and 2. The coordination sphere is completed by three chelating DME ligands, which results in a coordination number of eight.

The Ba–N distances are 2.749 and 2.752 Å. As for the Ca and Sr structures 1 and 2, these values are somewhat shorter than the bridging Ba–N distances (2.79 and 2.85 Å) in the bis[bis(tri-

**Table IV.** Calculated Relative Energies for Different Isomers of M(NH<sub>2</sub>)<sub>2</sub>(HF)<sub>4</sub> (M = Ca, Ba) at Various Theoretical Levels<sup>a</sup>

M		cis/stagg	cis/ecl	trans/stagg	trans/ecl
Ca	HF/B1//HF/B1	1.70	0.82	0.00	0.28
	HF/B2//HF/B1	1.20	0.09	0.00	0.22
	MP2/B2//HF/B1	1.17	0.00	0.43	0.71
Ba	HF/B1//HF/B1	1.25	0.00	4.11	3.16
	HF/B2//HF/B1	1.22	0.00	3.45	2.38
	MP2/B2//HF/B1	1.23	0.00	4.22	2.84

<sup>a</sup> B1 stands for the smaller basis sets, B2 for the extended basis sets (cf. computational details section). Thus, e.g., the notation MP2/B2//HF/B1 corresponds to an MP2 single-point calculation with B2 at the Hartree–Fock geometry optimized with B1.

methylsilyl)amide] dimer {Ba[N(SiMe<sub>3</sub>)<sub>2</sub>]<sub>2</sub>}.<sup>14</sup> The bond lengths to the six oxygens of the DME ligands range from 2.803 to 2.935 Å. The cisoid carbazole units are twisted as they are in 1 and in 2. While small covalent  $\pi$ -bonding contributions in this case probably would slightly favor an in-plane arrangement of the two carbazole rings,<sup>4</sup> steric effects apparently require the observed partial out-of-plane twisting. The N(1)–Ba–N(2) angle is only 98.1°. Even for this largest of the group 2 dications employed, no multihapto bonding is found. Table II gives the fractional coordinates and isotropic temperature factors compared with those of 1 and 2. Table III contains a summary of crystallographic data for 1, 2, and 3.

**The Model Complexes M(NH<sub>2</sub>)<sub>2</sub>(HF)<sub>4</sub> (M = Ca, Ba).** The origin of the cisoid position of the carbazole anions in the barium complex 3 compared to the transoid arrangement in the calcium and strontium complexes 1 and 2 has been investigated by ab initio calculations on the six-coordinate model systems M(NH<sub>2</sub>)<sub>2</sub>(HF)<sub>4</sub> (M = Ca, Ba). The energy differences between cis and trans NH<sub>2</sub>–M–NH<sub>2</sub> arrangements for the calcium model complex (cf. Figure 2) generally are very small (<1 kcal/mol, cf. Table IV). While the trans/staggered isomer (Figure 2d) is the most stable at the HF level, the cis/eclipsed isomer (Figure 2a) is slightly lower

**Table V.** Occupations of Metal ( $n-1$ )d- and  $ns$ -Orbitals for Two Model Complexes and for  $\text{Ba}(\text{NH}_2)_2$  in Different Conformations<sup>a</sup>

NAO	$\text{Ba}(\text{NH}_2)_2$		$\text{Ba}(\text{NH}_2)_2\text{-}(\text{HF})_4^b$		$\text{Ca}(\text{NH}_2)_2\text{-}(\text{HF})_4^b$	
	$C_{2v}^b$	$D_{2h}^c$	cis	trans	cis	trans
$ns$	0.016	0.006	0.032	0.030	0.077	0.073
$(n-1)d_{xy}$	0.035	0.000	0.023	0.026	0.019	0.021
$(n-1)d_{xz}$	0.016	0.042	0.010	0.003	0.007	0.000
$(n-1)d_{yz}$	0.045	0.000	0.030	0.018	0.021	0.001
$(n-1)d_{x^2-y^2} + (n-1)d_{z^2}$	0.018	0.022	0.014	0.019	0.015	0.024
$(n-1)d_{tot}$	0.114	0.064	0.077	0.066	0.062	0.045

<sup>a</sup>Natural population analysis was used (ref 24). The small p-populations (<0.006) have been neglected. HF/B2//HF/B1 results. <sup>b</sup>In-plane/eclipsed geometries. <sup>c</sup>The principal axes for  $D_{2h}$  symmetry have been chosen to match the  $C_{2v}$  orientation.

in energy at the MP2 level. The trans isomers exhibit nearly ideal octahedral structures with all N–Ca–N and F–Ca–F angles close to 180° (Figure 2c,d). This is consistent with the very regular structure of the calcium carbazole complex **1** (Figure 5).

The barium complex behaves quite differently: The cis/eclipsed isomer (Figure 3a), generally the most stable structure, is stabilized by ca. 3 kcal/mol (Table IV) with respect to the trans/eclipsed isomer (Figure 3c). Even when a trans structure is imposed (Figure 3c,d), no regular octahedral geometry results: the N–Ba–N and F–Ba–F angles are computed to be significantly smaller than 180° (particularly in the eclipsed in-plane isomer, Figure 3c). This indicates the preference of barium for a bent arrangement of the two anionic groups. The N–Ba–N angle in unsolvated  $\text{Ba}(\text{NH}_2)_2$  (calculated with a 6s6p5d-valence basis on Ba, DZ+P-valence basis on N, and DZP basis on H<sup>+</sup>) is ca. 118° for the eclipsed in-plane structure corresponding to Figure 3a. The linearization energy calculated for “naked”  $\text{Ba}(\text{NH}_2)_2$  is ca. 7 kcal/mol, whereas  $\text{Ca}(\text{NH}_2)_2$  is quasilinear.<sup>4</sup>

In all cases with nonlinear N–M–N units (Figure 2a,b, Figure 3), the eclipsed arrangement of the  $\text{NH}_2$ -groups with the hydrogens in the N–M–N plane is ca. 1 kcal/mol more stable than the staggered isomer. The staggered geometry is slightly more stable only for the trans structures of the calcium complex. Exactly the same conformational behavior was noted for the unsolvated diamides.<sup>4</sup> The M– $\text{NH}_2$  rotational barriers have been attributed to  $\pi$ -donor–acceptor bonding contributions between nitrogen  $\pi$ -lone-pairs and suitable empty metal d-orbitals.<sup>4</sup> The conformational preferences in these model systems indicate that small covalent contributions to the bonding in solvated compounds of Ca, Sr, or Ba also are important.

Table V compares the “natural population analysis” (NPA)<sup>12</sup> metal valence occupations for the eclipsed cis and trans structures of the two model complexes and for  $\text{Ba}(\text{NH}_2)_2$ .<sup>4</sup> The solvated barium complex exhibits larger s- and smaller d-populations than “naked”  $\text{Ba}(\text{NH}_2)_2$  (cf. Table V). This may be due to the somewhat smaller metal charges in the solvated species (the HF-ligands bear a small positive charge), as the atomic (or cationic) s–d promotion gap increases with decreasing metal charge. More importantly, Table V shows that the relative populations of the different d-orbitals in the barium complex are very similar to those found previously for unsolvated  $\text{Ba}(\text{NH}_2)_2$ . Thus, similar covalent bonding contributions are present, and the reasons for the cis preference in the solvated complex are likely to be the same as those responsible for the bent structure of  $\text{Ba}(\text{NH}_2)_2$ . However, the cis–trans energy difference of ca. 3 kcal/mol in the model complex is significantly reduced compared to the linearization energy (ca. 7 kcal/mol<sup>4</sup>) for  $\text{Ba}(\text{NH}_2)_2$ . Several effects may contribute to this reduction in the solvated species: The smaller metal charge and the corresponding smaller d-populations (cf. Table V) may diminish the contributions from covalent d-orbital participation (and a slightly less contracted metal d-basis was used for the unsolvated system<sup>4</sup>). Moreover, some N–Ba–N bending is present even in the trans complex (cf. Figure 3c,d). This also reduces the cis–trans energy difference.

**Table VI.** Calculated Metal–Ligand Distances (Å) and Relative Stabilities  $\Delta E$  (kcal/mol) of Mono- and Multihapto Model Systems  $\text{XM}^+\text{po}^-$  ( $\text{po}^- = \text{Pyrrolyl Anion}, \text{C}_4\text{H}_4\text{N}^-$ )<sup>a</sup>

$\text{XM}^+$	monohapto		multihapto		$\Delta E^a$
	R–MN	R–XM	R–M(ring) <sup>b</sup>	R–XM	
$\text{Na}^+$	2.165 (2.194)		2.276 (2.281)		5.4 (5.6)
$\text{K}^+$	2.533 (2.500)		2.708 (2.596)		6.6 (9.8)
$\text{Cs}^+$	2.792 (2.750)		3.001		6.7
$\text{Ca}^{++}$	2.251		2.424		5.6
$\text{Ba}^{++}$	2.545		2.784		7.4
$\text{HCa}^+$	2.278 (2.265)	2.074	2.414 (2.336)	2.062	10.6 (14.2)
$\text{FCa}^+$	2.282	2.024	2.406	2.018	11.7
$\text{HBa}^+$	2.564 (2.506)	2.362	2.817	2.429	8.8 (12.3)
linear <sup>c</sup>	2.638 (2.586)	2.459			14.0 (18.9)

<sup>a</sup>HF results with MP2 values in parentheses. The multihapto arrangement is generally the most stable. <sup>b</sup>For the multihapto structures, the M–(ring midpoint) distances are given. <sup>c</sup> $C_{2v}$  structure with H–Ba–N angle fixed to 180° (cf. Figure 4c).

The s-populations for the calcium complex are higher and the d-populations slightly lower than for the barium system (Table V). The reduced d-orbital occupation and the smaller polarizability of  $\text{Ca}^{2+}$  are two reasons for the smaller bending tendencies in calcium  $\text{MX}_2$  compounds compared to the barium species.<sup>1–5</sup> The lack of either a clearcut cis or trans preference in the solvated calcium model complex may also be due to these factors. However, our study of the group 2 dihalides<sup>3</sup> showed that the shorter metal–ligand distances in the calcium complexes lead to more severe anion–anion repulsion than those for the larger metals. This is probably the main reason for the trans preferences of the  $\text{CaX}_2(\text{L})_n$  structures ( $n > 3$ ).

**Results of ab Initio Model Calculations on  $\text{XM}^+\text{po}^-$**  ( $\text{XM}^+ = \text{Na}^+, \text{K}^+, \text{Cs}^+, \text{Ca}^{++}, \text{Ba}^{++}, \text{HCa}^+, \text{FCa}^+, \text{HBa}^+$ ;  $\text{po}^- = \text{Pyrrolyl Anion}$ ). The results of the Hartree–Fock geometry optimizations for the monohapto and multihapto structures of  $\text{BaH}^+\text{po}^-$  are shown in Figure 4. Table VI summarizes the HF and MP2 metal–ligand distances and multihapto vs monohapto stabilities for the complete series of calculated pyrrolyl-complex structures.

The H–Ba–N angle for the monohapto structure of  $\text{HBa}^+\text{po}^-$  is ca. 124° (cf. Figure 4c). The HF (MP2) stabilization energy compared to the restricted  $C_{2v}$  structure (H–Ba–N angle fixed at 180°, Figure 4b) is ca. 5.2 (6.6) kcal/mol. This is significant and compares well with the corresponding HF linearization energies obtained for  $\text{Ba}(\text{NH}_2)_2$  (ca. 6.6 kcal/mol)<sup>4</sup> and for  $\text{BaH}_2$  (ca. 4.9 kcal/mol).<sup>1</sup> The Ba–H and Ba–N distances lengthen considerably (by ca. 9.7 and 7.4 pm at the HF-level, cf. Table VI) when the H–Ba–N angle is forced to be 180°. This lengthening has been observed earlier for smaller  $\text{MX}_2$  species.<sup>1–4</sup> These results clearly indicate that the bending effects for a barium dication bound monohapto to the nitrogen atoms of an organic amide like pyrrole or carbazole are similar to those for simpler  $\text{BaX}_2$  systems like  $\text{Ba}(\text{NH}_2)_2$ .<sup>4</sup>

For all of these unsolvated species, the multihapto coordination mode is clearly favored over  $\sigma$ -binding to nitrogen (cf. Table VI). As the bond contractions for the heavier metals caused by correlation effects are much larger for the multihapto arrangement, correlation generally increases the observed multihapto preference (the unusually large bond contractions due to electron correlation for these and other heavy-metal cations bound to the  $\pi$ -faces of delocalized systems, such as the cyclopentadienyl anion, are well-known<sup>5,26,27</sup>). While the MP2 energy differences are probably more reliable than the HF values, the changes due to correlation are almost the same in all cases (except for  $\text{XM}^+ = \text{Na}^+$ , where only valence correlation was considered) and do not affect the general trends.

(26) For calculations on transition metal metallocenes, see: Lüthi, H. P.; Ammeter, J. H.; Almlöf, J.; Faegri, K. *J. Chem. Phys.* **1982**, *77*, 2002. Almlöf, J.; Faegri, K.; Schilling, B. E. R.; Lüthi, H. P. *Chem. Phys. Lett.* **1984**, *106*, 266. Lüthi, H. P.; Siegbahn, P. E. M.; Almlöf, J.; Faegri, K.; Heiberg, A. *Chem. Phys. Lett.* **1984**, *111*, 1. Park, C.; Almlöf, J. *J. Chem. Phys.* **1991**, *95*, 1829.

(27) Calculations on the alkali metal cyclopentadienides also indicate large correlation effects on M–Cp distances: Lambert, C.; Kaupp, M.; Schleyer, P. v. R. To be published.



The energy differences between mono- and multihapto binding show the expected increase from Na to Cs, but the values for  $\text{XM}^+ = \text{HBa}^+$  are smaller than those for  $\text{HCa}^+$  due to the bending in the barium monohapto structure (Table VI). The multihapto preferences of the alkali systems are not greater than those of the group 2 fragments with comparable ionic radii<sup>28</sup> ( $\text{Na}^+$  vs  $\text{Ca}^{2+}$ ,  $\text{K}^+$  vs  $\text{Ba}^{2+}$ ). Indeed, while the  $\text{Ca}^{2+}$  and  $\text{Ba}^{2+}$  radical cations give rise to energy differences similar to those of  $\text{Na}^+$  and  $\text{K}^+$ , the more realistic  $\text{HCa}^+$ ,  $\text{FCa}^+$ , and  $\text{HBa}^+$  model species yield even considerably higher values. This is due to the larger charge transfer for these fragments. Thus, the experimental observation<sup>6</sup> of M–C contacts in the dimeric potassium complex (*N*-carbazolyl)K(PMDTA) (PMDTA = *N,N,N',N'',N'''*-pentamethyldiethylenetriamine) and the absence of M–C binding in the barium complex 3 (Figure 7) are not due to any inherent trends in the multihapto vs monohapto coordination preferences of the “naked”  $\text{XM}^+$  fragments.

The internal coordinates of the pyrrole anion for a given coordination mode differ by less than 0.005 Å and 0.5° for all  $\text{XM}^+$  fragments. This is consistent with predominantly ionic bonding (confirmed by the NPA<sup>24</sup> charges). In the multihapto structures (cf. Figure 4a), the  $\text{XM}^+$  fragment generally is located approximately above the midpoint of a line connecting C1 and C2. The pyrrole hydrogen atoms are slightly (by ca. 3–4°) bent away from the metal fragment.<sup>5</sup> The hydride and fluoride ions in the multihapto structures of  $\text{XM}^+\text{po}^-$  ( $\text{XM}^+ = \text{HCa}^+$ ,  $\text{FCa}^+$ ,  $\text{HBa}^+$ ) are located close to a line through the metal and the midpoint between C1 and C2 (cf. Figure 4a).

### General Discussion

The heavy alkaline-earth metal carbazole complexes 1–3 all crystallize as monomers, in contrast to the corresponding dimeric alkali metal complexes.<sup>6</sup> As *ab initio* calculations on the  $(\text{HMNH}_2)_2$  ( $\text{M} = \text{Ca}, \text{Sr}, \text{Ba}$ ) and  $(\text{MNH}_2)_2$  ( $\text{M} = \text{K}, \text{Rb}, \text{Cs}$ ) systems give larger dimerization energies for the group 2 amides,<sup>29</sup> the monomeric nature of complexes 1–3 is most certainly due to the presence of the two bulky carbazole anions for each metal dication. Interestingly, the  $\text{N}(\text{SiMe}_3)_2^-$  anions, which are also quite large but have a more three-dimensional shape, may give rise either to monomeric or to dimeric solid-state structures with  $\text{Ca}^{2+}$  or  $\text{Ba}^{2+}$ , depending on the conditions of preparation.<sup>12,14</sup>

The metal coordination numbers increase smoothly from six in the calcium complex 1 to seven in the strontium derivative 2 to eight in the barium complex 3 (cf. Figures 5–7). However, there is a sharp discontinuity in the ligand orientation: While the carbazole anions are transoid for the calcium and strontium systems (with N–M–N angles of 172.7 and 173.1°, respectively), the anions are cisoid in the barium complex 3 (with an N–Ba–N angle of ca. 98.1°). Our *ab initio* calculations of the model complexes  $\text{M}(\text{NH}_2)_2(\text{HF})_4$  (see above) reveal the electronic origin of these differences (Tables IV and V). A bent amide–barium–amide arrangement is favored due to the small but significant covalent  $\sigma$ -bonding contributions involving metal d-orbitals<sup>4</sup> (polarization of the metal cation by the anions also plays a role<sup>1,3</sup>). This not only is true for “naked” diamides,  $\text{M}(\text{NH}_2)_2$ ,<sup>4</sup> but also is true when additional, more loosely bound neutral coligands are present (less symmetrical arrangement of the neutral coligands in the cisoid structure also may contribute to this preference<sup>30</sup>). We state this as a general conclusion: *As anionic ligands are bound more strongly than neutral coligands, the preferred anion orientation in unsolvated species will dominate the coordination geometries of the solvated complexes as well.* Exceptions are likely to be found when the neutral coligands are bulky.

(28) Shannon, R. D. *Acta Crystallogr. A* 1976, A32, 751.

(29) MP2 calculations with extended basis sets yield dimerization energies of ca. 46.8, 42.5, and 35.9 kcal/mol for  $\text{KNH}_2$ ,  $\text{RbNH}_2$ , and  $\text{CsNH}_2$ , respectively (cf. ref 6a). The corresponding dimerization energies for  $\text{NCaNH}_2$ ,  $\text{HSrNH}_2$ , and  $\text{HBaNH}_2$  are ca. 63.5, 60.0, and 44.2 kcal/mol (Kaupp, M. Dissertation, Universität Erlangen-Nürnberg, 1992).

(30) *Ab initio* calculations indicate the complexes  $\text{Ba}^{2+}(\text{L})_n$  ( $\text{L} = \text{H}_2\text{O}, \text{NH}_3$ ) to prefer bent ( $n = 2$ ) or pyramidal ( $n = 3$ ) structures: Kaupp, M.; Schleyer, P. v. R. *J. Phys. Chem.*, in press.

The computational results for the model complex  $\text{HBa}^+\text{po}^-$  ( $\text{po}^- = \text{pyrrole anion}$ ) (Table VI and Figure 4) indicate that the parent fragment  $\text{Ba}(\text{NH}_2)_2$  is a reasonable model for the linearization energies and bending angles of other  $\sigma$ -bound barium amides. Thus, the ca. 3 kcal/mol preferences for cis over trans structures of  $\text{Ba}(\text{NH}_2)_2(\text{HF})_4$  should be a good measure of the electronic contributions to the cisoid structure in the barium carbazole complex 3. A cisoid–transoid energy difference of only 2 kcal/mol would account for more than a 95:5 equilibrium ratio in favor of the cisoid isomer at room temperature.

One referee argued that the observed structure of the barium complex 3 may be due to a more favorable arrangement of the DME ligands. However, it is by no means obvious why a cisoid position of the carbazole anions should decrease the steric ligand–ligand interactions. Instead, the repulsion of the carbazole anions (which bear an appreciable negative charge) will be considerably larger in the cisoid structure. There are no short intermolecular contacts in the crystal structures of the monomeric complexes 1, 2, and 3. However, crystal-packing contributions are difficult to exclude completely. Hence, the solution structure of barium carbazole would be of interest but is hard to obtain experimentally.

The only other structurally characterized monomeric examples of  $\text{BaX}_2(\text{L})_n$  species (with only monodentate anions) known to us are complexes of  $\text{Ba}(\text{NCS})_2$  with macrocyclic polyether ligands.<sup>31</sup> While the anionic isothiocyanate ligands in these barium complexes (and in related strontium derivatives<sup>32,33</sup>) are in cisoid position on one side of the macrocycle, a related calcium complex features transoid NCS ligands.<sup>33</sup> Interestingly, the benzoxazolyl nitrogens are cisoid in the X-ray structure of monomeric (2-mercaptobenzoxazole)<sub>2</sub>Ba(HMPTA)<sub>3</sub> [HMPTA =  $\text{O}=\text{P}(\text{NMe}_2)_3$ ] but they are transoid in (2-mercaptobenzoxazole)<sub>2</sub>Ca(HMPTA)<sub>2</sub>(H<sub>2</sub>O)<sub>2</sub>.<sup>15</sup> However, the additional Ba–S interactions, present in the cisoid complex, complicate the analogy.

Why do the potassium, rubidium, and cesium carbazole complexes exhibit interactions to the  $\pi$ -face of the ligand<sup>6</sup> while the Ca, Sr, and Ba complexes do not? The dimeric nature of the alkali metal derivatives and the carbazole anion bridging<sup>6</sup> offer the possibility of amide  $\pi$ -system interactions, even when no particularly short M–C contacts are present. Thus, the group 1 and group 2 systems are not directly comparable. Due to its large size, the barium dication might be expected to be the best alkaline-earth metal candidate for multihapto bonding. However, as shown by the calculations on  $\text{HBa}^+\text{pyrrole}^-$  (Table VI, Figure 4), the stabilization of the cisoid monohapto structure by covalent  $\sigma$ -bonding contributions and by cation polarization (no significant stabilization of this type occurs for the multihapto bonding mode<sup>2</sup>) reduces the multihapto preference in the unsolvated model complex. The energy differences between possible multihapto structures of solvated barium carbazole complexes and the monohapto structure (3) actually observed (Figure 7) are unknown. A complete dissection of the monohapto vs multihapto preferences would have to include consideration of crystal-packing effects (although the monomeric units in the solid-state structures of 1–3 are well-separated) and ligand–ligand steric interactions, as well as the observed electronic stabilization of cisoid  $\text{BaX}_2(\text{L})_n$  arrangements with  $\sigma$ -bound ligands X (cf. Table IV).

### Conclusions

The questions posed in the introduction may be answered as follows:

(i) The Ca, Sr, and Ba carbazole complexes 1, 2, and 3 are all monomeric, due to the presence of two bulky carbazole anions per metal cation.

(31) See, e.g.: Weber, G. *Inorg. Chim. Acta* 1981, 58, 27. Allwood, B. L.; Fuller, S. E.; Ning, P. C. Y. K.; Slawin, A. M. Z.; Stoddart, J. F.; Williams, D. J. *J. Chem. Soc., Chem. Commun.* 1984, 1356.

(32) Fenton, D. E.; Cook, D. H.; Nowell, I. W.; Walker, P. E. *J. Chem. Soc., Chem. Commun.* 1977, 623.

(33) Fenton, D. E.; Cook, D. H.; Nowell, I. W.; Walker, P. E. *J. Chem. Soc., Chem. Commun.* 1978, 279.

(ii) The metal coordination numbers vary regularly with cation size. They are six with Ca, seven with Sr, and eight with Ba.

(iii) The orientation of the carbazole anions is transoid with Ca and Sr but cisoid with Ba. We expect these structural trends to be general. Calculations on the model complexes  $M(\text{NH}_2)_2\text{-(HF)}_4$  ( $M = \text{Ca}, \text{Ba}$ ) indicate that the involvement of metal d-orbitals in small covalent bonding contributions (and probably cation polarization) is responsible for the cisoid anion arrangement in the Ba complexes. Anion-anion repulsion probably is the major factor that prevents similar structures for the Ca and Sr systems. These results relate the structures of the solvated complexes **1**, **2**, and **3** (transoid vs cisoid) to those of "naked"  $\text{MX}_2$  species<sup>1-5</sup> (linear vs bent). Further related experimental examples<sup>15,31-33</sup> have been discussed.

(iv) In contrast to the X-ray structures of the heavier alkali metal carbazoles, which exhibit varying degrees of multihapto bonding to the carbazole  $\pi$ -system,<sup>6</sup> the alkaline earth metals in **1**, **2**, and **3** are exclusively  $\sigma$ -bound to the carbazole nitrogen atoms. Model calculations on unsolvated complexes of the pyrrolyl anion with the alkali and alkaline earth cations show, in contrast, that the alkaline earth metals should have an even greater multihapto preference than the group 1 metals. However, due to the dimeric nature of the alkali metal carbazole complexes,<sup>6</sup> the two sets of structures are not strictly comparable.

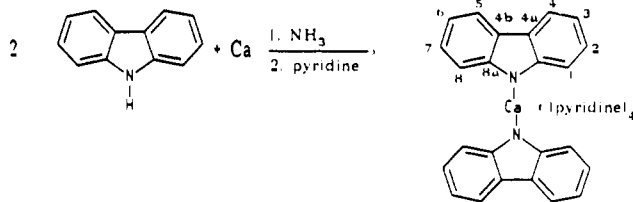
The present experimental and computational results for solvated complexes agree with previous conclusions based on simple  $\text{MX}_2$  species of Ca, Sr, and Ba.<sup>1-5</sup> In addition to Coulombic interactions, small covalent bonding contributions involving metal d-orbitals and the high polarizability of the metal cations are important in determining the structural preferences of heavy alkaline-earth metal coordination compounds. The structures of barium compounds are generally expected to be less symmetrical than those of the corresponding calcium species (Sr compounds should be intermediate).

## Experimental Section

All manipulations were carried out under argon atmosphere by using Schlenk techniques. DME was distilled from Na/K alloy under argon atmosphere. Pyridine was dried and distilled from KOH under argon. Calcium, strontium, and barium were used as dendritic metals. Nuclear magnetic resonance spectra were run on a Jeol JNM-GX-400 spectrometer at 27 °C (operating at 400 MHz for <sup>1</sup>H and 100 MHz for <sup>13</sup>C). The <sup>1</sup>H- and <sup>13</sup>C-NMR spectra were referenced to TMS.

**(N-Carbazolyl)<sub>2</sub>Ca(pyridine)<sub>4</sub> (1).** Calcium (0.2 g, 5 mmol) was dissolved in 100 mL of liquid ammonia at -80 °C, and carbazole (1.67 g, 10 mmol) was added to the dark-blue solution while the mixture was stirred. On being warmed to -70 °C, the solution changed color and a white precipitate formed. After evaporation of the ammonia overnight, 50 mL of pyridine was added and the mixture was refluxed. The resulting orange-colored solution was cooled to -18 °C. The yellow microcrystalline product which formed after 1 day was filtered off, washed several times with hexane, and dried (yield 87% crude product). The microcrystalline material was dissolved in pyridine and covered carefully with a layer of hexane. After 1 week at room temperature, yellow rhombic crystals of X-ray quality were obtained. Anal. Calcd for  $\text{C}_{39}\text{H}_{51}\text{N}_9\text{Ca}$ : C, 76.51; H, 5.55; N, 13.61. Found: C, 76.87; H, 5.84; N, 13.43. <sup>1</sup>H-NMR ( $\text{C}_5\text{D}_5\text{N}$ ):  $\delta$  6.89 (d, H 1/8), 7.09 (t, H 3/6), 7.29 (t, H 2/7), 8.08 (d, H 4/5), 7.19, 7.57, 8.71 (pyridine). <sup>13</sup>C-NMR ( $\text{C}_5\text{D}_5\text{N}$ ):  $\delta$  114.94 (C 3/6), 116.66 (C 1/8), 119.89 (C 4/5), 122.96 (C

2/7), 126.52 (C 4a/4b), 152.37 (C 8a/9a), 124.05, 136.03, 150.31 (pyridine).



**1**

**(N-Carbazolyl)<sub>2</sub>Sr(NH<sub>3</sub>)(DME)<sub>2</sub> (2).** The reaction of strontium with carbazole was carried out as described for **1** using 5 mmol of strontium and 10 mmol of carbazole. After evaporation of the ammonia, 10 mL of DME was added. This gave a white suspension, which was dissolved in 10 mL of pyridine to form an orange-colored solution. After 3 days at room temperature, crystallization yielded colorless crystals of X-ray quality (yield 53% of pure product). Anal. Calcd for  $\text{C}_{32}\text{H}_{39}\text{N}_5\text{O}_4\text{Sr}$ : C, 62.23; H, 6.37; N, 6.81. Found: C, 62.19; H, 6.42; N, 6.85. <sup>1</sup>H-NMR ( $\text{C}_5\text{D}_5\text{N}$ ):  $\delta$  1.44 (s,  $\text{NH}_3$ ), 3.26 (s,  $-\text{O}-\text{CH}_3$ , DME), 3.49 (s,  $-\text{O}-\text{CH}_2-$ , DME), 7.26 (t, t, H 2/7, H 3/6), 7.70 (d, H 1/8), 8.58 (d, H 4/5). <sup>13</sup>C-NMR ( $\text{C}_5\text{D}_5\text{N}$ ):  $\delta$  58.66 ( $-\text{O}-\text{CH}_3$ , DME), 72.06 ( $-\text{O}-\text{CH}_2-$ , DME), 114.87 (C 3/6), 115.37 (C 1/8), 120.36 (C 4/5), 123.46 (C 2/7), 126.24 (C 4a/4b), 152.6 (C 8a/9a).

**(N-Carbazolyl)<sub>2</sub>Ba(DME)<sub>3</sub> (3).** The reaction of 5 mmol of dendritic barium with 10 mmol of carbazole was carried out as described for **1** and **2**. After 4 days, colorless rhombic crystals of X-ray quality were obtained from a 1:1 mixture of DME and pyridine (yield 52% of pure product). Anal. Calcd for  $\text{C}_{36}\text{H}_{46}\text{N}_5\text{O}_6\text{Ba}$ : C, 58.42; H, 6.26; N, 3.78. Found: C, 58.19; H, 6.32; N, 3.82. <sup>1</sup>H-NMR ( $\text{C}_5\text{D}_5\text{N}$ ):  $\delta$  3.25 (s,  $-\text{O}-\text{CH}_3$ , DME), 3.48 (s,  $-\text{O}-\text{CH}_2-$ , DME), 7.28 (t, t, H 2/7, H 3/6), 7.77 (d, H 1/8), 8.60 (d, H 4/5). <sup>13</sup>C-NMR ( $\text{C}_5\text{D}_5\text{N}$ ):  $\delta$  58.63 ( $-\text{O}-\text{CH}_3$ , DME), 72.06 ( $-\text{O}-\text{CH}_2-$ , DME), 114.75 (C 3/6), 114.97 (C 1/8), 120.45 (C 4/5), 123.50 (C 2/7), 126.24 (C 4a/4b), 152.44 (C 8a/9a).

Suitable crystals of **1**, **2**, and **3**, obtained through slow crystallisation from pyridine/DME, were sealed into capillaries under argon and mounted on the diffractometer. Initial investigation revealed all the crystal systems to be monoclinic. Final lattice parameters were determined from least square refinement of the angular settings of 18 intense, accurately centered reflections. The data were corrected for crystal decay and Lorentz and polarization effects and converted into structure factors. No absorption correction was applied. All three structures were solved with direct methods. In **1** and **3** all non-hydrogen atoms were refined anisotropically. In **2**, N(2), O(1), O(2), and some carbon atoms could not be refined anisotropically.

**Acknowledgment.** This work was supported by the Deutsche Forschungsgemeinschaft, the Fonds der Chemischen Industrie, the Volkswagenstiftung, and the Convex Computer Corporation. M.K. acknowledges a Kékulé scholarship by the Fonds der Chemischen Industrie. We are particularly grateful to the theoretical chemistry group in Stuttgart for providing pseudopotentials and basis sets prior to publication (cf. ref 16 and 21a).

**Supplementary Material Available:** For compounds **1-3**, tables of crystallographic details, isotropic and anisotropic thermal parameters, and complete bond distances and angles (8 pages); listings of calculated and observed structure factors (20 pages). Ordering information is given on any current masthead page.